Flame Inhibition of Aluminum Dust Explosion by Sodium Bicarbonate with different particle size

Haipeng Jiang, Wei Gao*
School of Chemical Engineering, Dalian University of Technology
Dalian, Liaoning, China

1 Introduction

Aluminum flame has extremely high temperature and fast flame speed, which can cause seriously thermal damages and pressure built-up. A considerable number of severe aluminum dust explosion accidents have taken place in recent years, in which many people have lost their lives [1]. Therefore, it is significant and necessary to clearly and scientifically understand the flame inhibition mechanism of aluminum dust to provide a safe manufacturing and processing environment. Sodium bicarbonate ($NaHCO_3$; also known as SBC), as a chemical inhibitor, exhibits excellent efficiency of flame extinguish by catalytic recombination of key flame radicals. Therefore, $NaHCO_3$ particles have a certain explosion inhibition performance for aluminum flame. However, few researchers have studied the effect of particle size on flame inhibition efficiency. In this study, the inhibition efficiency of $NaHCO_3$ with various particle sizes on flame propagation of aluminum dust cloud is determined systematically. The effect of $NaHCO_3$ on flame morphology and flame propagation velocity of 5 μm aluminum dust is investigated. To reveal the suppression mechanism in detail, a tentative kinetic model considering both gas and surface chemistry is first developed. The effect of SBC on gas and surface reaction of aluminum particles burning is further discussed.

2 Experimental

Experimental apparatus (Fig. 1) and methods were similar to our previous study [2]. The dispersion pressure is 0.46 MPa. The ignition delay time is 0.9 s. The discharge duration is 0.25 s. Photron SA4 high-speed video camera with normal lens (Nikkor 50 mm f/1.2, Nikon) and a microscopic lens (AF Micro Nikkor 200 mm f/4D, Nikon) is used to record flame propagation and flame microstructures at 10,000 frames per second.

5μm aluminum particles are selected as the experimental samples. The nominal concentration of aluminum dust in this study is 1000 g/m^3. Analytically pure $NaHCO_3$ powder is chosen as inhibitor in experiments. The $NaHCO_3$ powder is sifted into three particle size distributions of 53–75 μm, 75–100 μm, and 100–212 μm.

Correspondence to: gaoweidlut@dlut.edu.cn

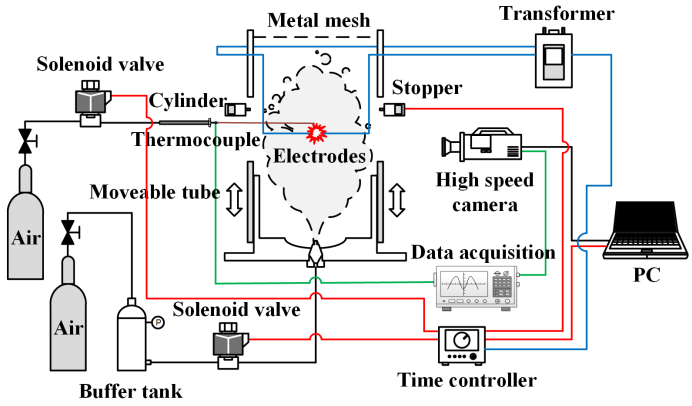

Figure 1. Experiment apparatus

3 Kinetics

This paper deals with nascent 5 μm aluminum particles by ignoring the presence of the alumina shell. Both gas and surface reactions of aluminum combustion were considered in the numerical model. A detailed description of the gas–phase mechanism is given by Gao [2]. Surface chemistry of aluminum particles combustion considering surface and gas/surface interactions is developed based on the previous work of Glorian et al. [3]. Surface chemistry considers species on the top layer of the solid. In this study, species are adsorbed on the open sites Al(L) of the aluminum surface. Surface site species and bulk-phase species are noted using suffixes (S) and (B), respectively. For example, O + Al(L) → O(S) + Al(B) means that O atom is absorbed on aluminum surface and occupied a free site Al(L) with the generation of adsorbate O(S). Then, the occupied site behaves like subsurface bulk aluminum. In the reverse reaction O(S) + Al(B) → O + Al(L), the adsorbate O(S) left the aluminum surface and the bulk aluminum Al(B) becomes an free site Al(L). 0–D Homogeneous reactor in CHEMKIN–PRO is used. According to previous study, liquid alumina models as a gaseous phase, even though it had large mass fraction but little volume fraction. Meanwhile, aluminum-oxide cap is not accounted for in present work. Note that condensed phase products are not considered. Initial pressure and initial temperature is 1 atm and 2700K. The mole ratio of N_2 and O_2 for air was 3.76. The inerting ratio (α) used in this part was referred to the molar concentration ratio of suppressant to gaseous–Al. To reveal flame inhibition mechanism of $NaHCO_3$ for aluminum flame, a detailed investigation of stoichiometric concentration (ϕ Al = 1) is performed.

4 Results and discussion

4.1 Flame morphology

Figure 2 shows a typical series of high–speed photomicrographs of aluminum flame doped with $NaHCO_3$ of different particle size. As shown in Fig. 2a, the flame morphology of 5μm Al dust cloud is regular and symmetric. The flame luminous intensity is strong. Figure 2b–2d show that the flame colour changes to intense yellow after the addition of $NaHCO_3$.

As shown in Fig. 3a, discrete gas phase flame can be found around 5μm Al particles. A gas–phase flame accompanying rapid evaporation of 5μm Al particles forms in the vicinity of the flame front. With the addition of $NaHCO_3$, the oxidizer components become a mixture of O_2, CO_2 and H_2O. As shown in Fig. 3b, aluminum flame diameter becomes closer to the surface after adding $NaHCO_3$. It can be seen that the

flame front of 5μm Al particles is close to the particle surface in CO_2 and H_2O. Meanwhile, the gas phase flame of aluminum dust is weakened by $NaHCO_3$ addition.

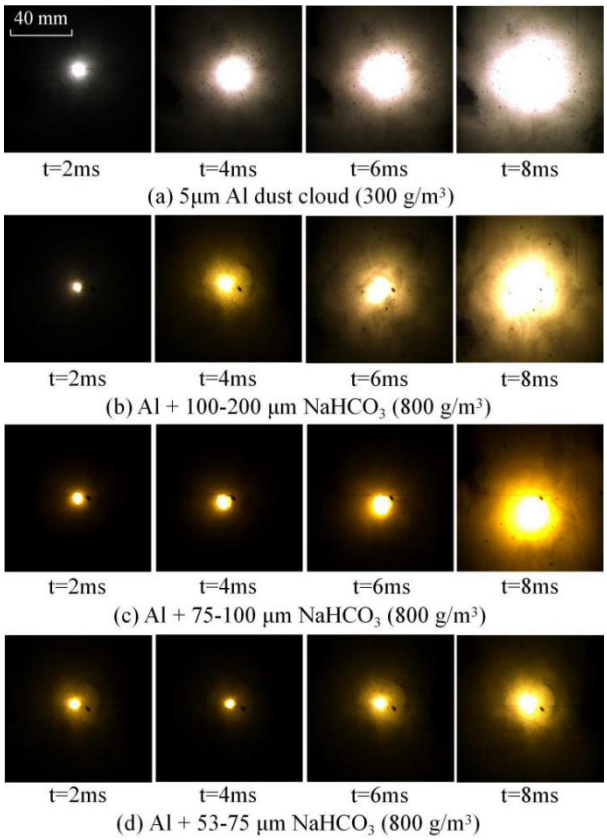

Figure 2. Flame propagations of 5μm aluminum dust cloud doped with sodium bicarbonate

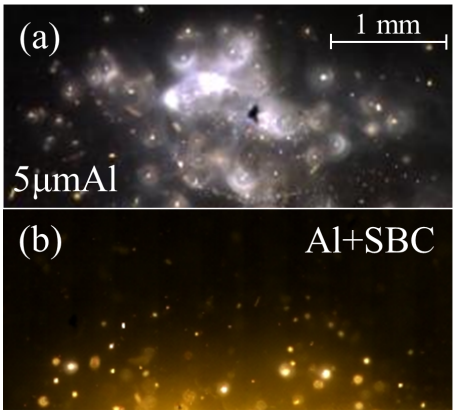

Fig. 3. Flame microstructures in (a) 5 μm Al and (b) 5 μm Al/$NaHCO_3$ mixture.

4.2 Flame propagation velocities

The flame edges are recognized through a MATLAB program based on the Roberts operator. The flame propagation velocity can be determined by examining the movement of the flame front. Flame contour on each frame was matched with an ellipse, since the flame is not always spherically symmetrical. The flame radius of undoped and doped Al/air mixture was calculated using the method in the literature [4]. Flame propagation velocity is derived from the flame radius vs. time. The distance from the flame front to the ignition point is evaluated by the most advanced point along the horizontal direction in the flame front.

As shown in Fig. 4a, for $NaHCO_3$ (SBC) addition, the time to reach the edge of combustion space is prolonged and increases with the particle size of SBC decreases. As shown in Fig. 4b, the average flame propagation velocity decreases with the addition of SBC. Fig. 5 plots the average flame propagation velocity of undoped and doped flames as a function of SBC concentration. Results show that the average flame propagation velocity decreases with increasing SBC concentration and decreasing SBC particle size. Hence, we can concluded that fine-size $NaHCO_3$ particles in the range studied exert a stronger inhibition efficiency for aluminum flame compared to coarse $NaHCO_3$ particles.

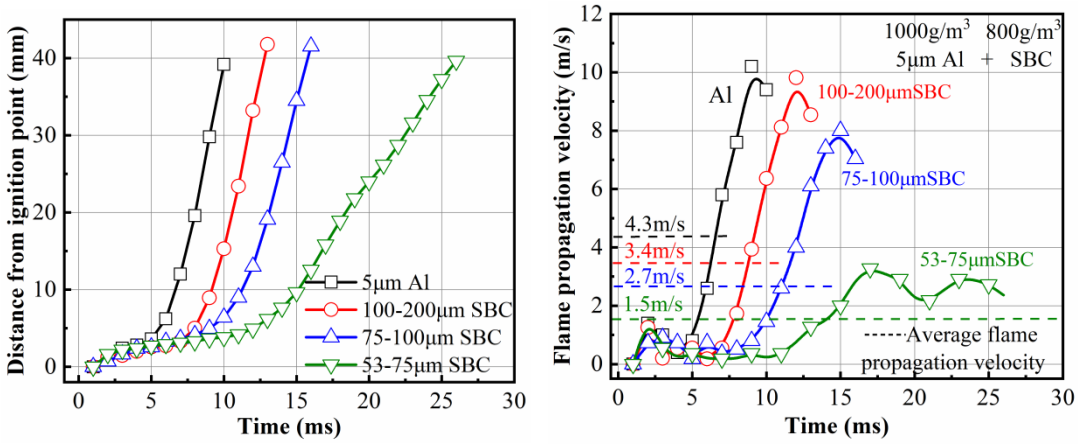

Figure 4. Flame front position and flame propagation velocity of 5 μm Al/SBC mixture.

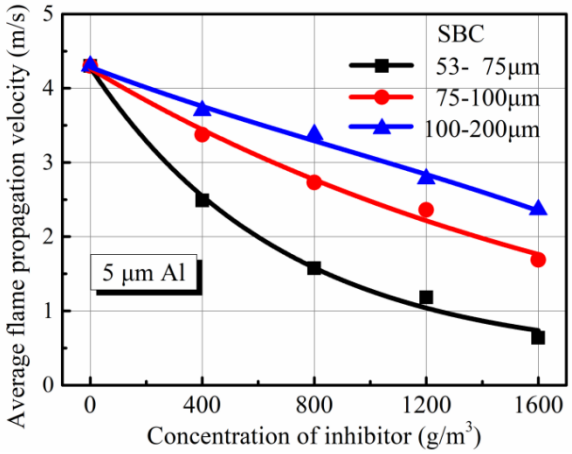

Figure 5. Average flame propagation velocity of 5 μm Al/SBC mixture (Al = 1000 g/m^3)

4.3 Inhibition mechanism

(1) Thermal effects

The inhibition mechanism for sodium bicarbonate occurs in four determinant steps. First, SBC particles undergo heating due to initiated aluminum combustion. Second, the SBC begins to decompose. Third, gas and solid phase decomposition products are produced. Fourth, chemical interaction with the flame. The total duration of these four events is designated by t_i. Chemical inhibition cannot be accomplished unless the sum of these four characteristic times (t_s) is shorter than the burning time (t_b) of an aluminum particle. This relationship can be expressed by

$$t_b \geq t_s = t_1 + t_2 + t_3 + t_4 \quad (1)$$

Meanwhile, the effectiveness of the physical effect depends on the ability of solid inhibitors to absorb heat. The endothermic decomposition process of solid particles is limited by the thermal relaxation timescale (τ_T) [5]:

$$\tau_T = \frac{m_p C_{Pp}}{\pi D_p \lambda_s Nu} \quad (2)$$

where D_p denotes particle diameter, λ_s is the thermal conductivity, C_{Pp} is specific heat at constant pressure, and Nu is the non-dimensional Nusselt number.

This suggests that the characteristic times of fine SBC particles are expected to be shorter compared with those of coarse ones, especially for the first three steps of the inhibition process. Therefore, fine SBC particles have a stronger inhibition efficiency.

(2) Gas phase inhibition mechanism

Our previous study reveals that $NaHCO_3$ appears to play a pivotal role in impeding gas phase aluminum combustion propagation. The chemical kinetic model indicates that the NaO ⇔ Na inhibition cycle is effective to reduce O atoms. Na-containing species consume O atoms and dilute intermediate AlO, which causes less heat release and a lower flame temperature. Meanwhile, the reduction of the concentrations of AlO and O in the reaction zone becomes larger with $NaHCO_3$ concentration increases.

(3) Surface reaction inhibition mechanism

In this study, the process of aluminum vaporization is described by reaction Al(B) + Al(L) = Al + Al(L) in the surface mechanism. The rate of surface reaction and Al particles vaporization is limited by the number of Al(L), since surface reaction considers species adsorbed on Al(L), and the adsorption capacity of the surface of aluminum particles and the number of Al(L) are limited. As shown in Fig. 6, Al(L) site fraction increases with inerting ratio of $NaHCO_3$ increases. Hence, the increase of $NaHCO_3$ concentration can decrease the rate of aluminum vaporization, which suppresses the surface reactivity at aluminum particle surface. Site fractions of AlO(S), AlO_2(S) and O(S) decrease with the increase of α of $NaHCO_3$. These results indicate that the diffusion rate of oxidizers close to the droplet surface is reduced by inhibitor addition.

Figure 7 shows the results of sensitivity analysis of Al(L) site fraction at α = 0.5, 1.0 and 2.0. Negative sensitivity coefficients represent a suppression effect on aluminum vaporization. As shown in Fig. 7, NaOH + O = NaO + OH and NaOH + OH = NaO + H_2O have the biggest negative sensitivity coefficient. Therefore, these reactions play a key role in surface reaction inhibition of aluminum particles.

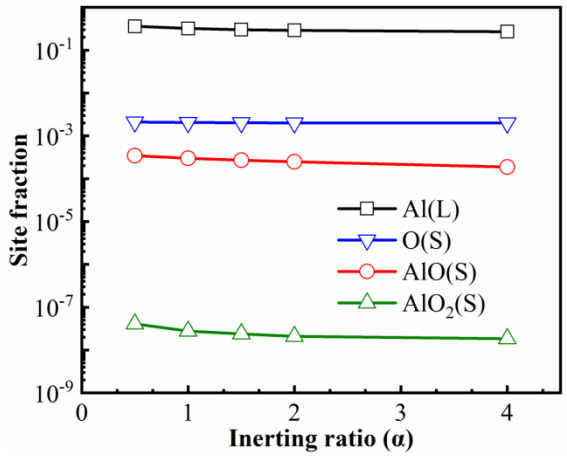

Figure 6. Occupied site fractions at aluminum surface as a function of inerting ratio in air

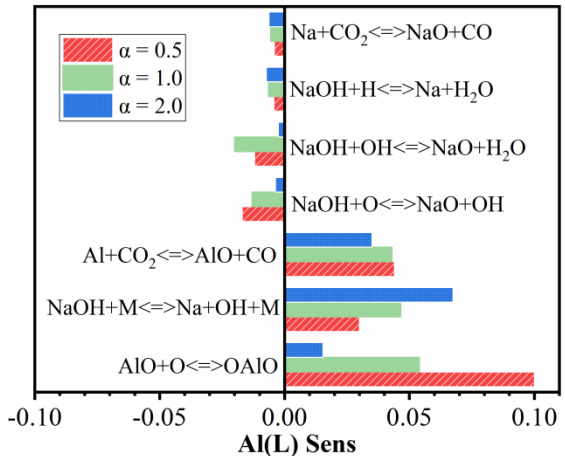

Figure 7. Sensitivity of Al(L) due to $NaHCO_3$ addition

5 Conclusions

Experimental and numerical investigation is conducted to reveal the inhibition mechanism of $NaHCO_3$ for aluminum flame. The effect of $NaHCO_3$ particle size on inhibition efficiency for aluminum flame is systematically discussed. The conclusions can be summarized as follows.

Flame morphology and flame colour change with the addition of $NaHCO_3$. The average flame propagation velocity decreases as the concentration of $NaHCO_3$ particles increases. Meanwhile, fine $NaHCO_3$ particles within the range studied have a greater reduction in average flame propagation compared to the coarser one. Hence, the inhibition efficiency depends on the particle size of $NaHCO_3$. The simulations indicate that decomposition products of $NaHCO_3$ particles reduce the burning rate of aluminum flame and obstruct complete metal oxidation of aluminum particles through flame radical diminution and AlO dilution. Additionally, the addition of $NaHCO_3$ can reduce the surface reaction rate, the vaporization rate of aluminum particles, and decrease the diffusion rate of oxidizers near Al droplet surface.

References

[1] Taveau J., Hochgreb S., Lemkowitz S., Roekaerts D. (2018). Explosion hazards of aluminum finishing operations, J. Loss Prevention Process Indust. 51: 84-93.

[2] Jiang H., Bi M., Li B., Ma D., Gao W. (2019). Flame inhibition of aluminum dust explosion by $NaHCO_3$ and $NH_4H_2PO_4$, Combust. Flame. 200: 97-114.

[3] Glorian J., Gallier S., Catoire L. (2016). On the role of heterogeneous reactions in aluminum combustion, Combust. Flame. 168: 378-392.

[4] Julien P., Vickery J., Goroshin S., Frost D., Bergthorson J. (2015). Freely-propagating flames in aluminum dust clouds, Combust. Flame. 162: 4241-4253.

[5] Cloney, C, Ripley, R, Pegg, M, Amyotte P. (2018). Laminar burning velocity and structure of coal dust flames using a unity Lewis number CFD model, Combust. Flame 190: 87-102.